Journal of Materials Chemistry B

RSC Publishing

COMMUNICATION

View Article Online
View Journal | View Issue

Carbon nanotubes for highly sensitive colorimetric immunoassay biosensor†

Cite this: *J. Mater. Chem. B*, 2013, **1**, 5389

Received 16th July 2013
Accepted 13th August 2013

DOI: 10.1039/c3tb20980f

www.rsc.org/MaterialsB

Jing-Huei Huang, Ying-Jhan Hong, Yun-Tzu Chang, Pin Chang and Tri-Rung Yew*

A colorimetric immunoassay biosensor is developed employing CNTs as a label material, which allowed direct observation of the sensing result by the naked eye. Implemented for HSA, the detection limit is 3 $\times$ 10^{-5} mg ml^{-1} when characterized using UV-Vis.

Immunoassay biosensors based on the specificity of antigen–antibody recognition reaction have become more and more important in clinical diagnostics and treatment.[1] Nowadays, a large number of studies have been focused on using the unique properties of nanomaterials to develop various novel nanostructure-based immunoassay biosensors such as electromechanical, electrical and mass-sensitive biosensor systems.[2,3] These biosensors exhibit high sensitivity, but the incorporated expensive sensing systems still limit their applications in daily life. One way to solve this issue is using ultraviolet-visible spectroscopy (UV-Vis) as the sensing system for optical biosensors.

In order to enhance the optical signal for UV-Vis detection, gold nanoparticles (AuNPs) have been extensively applied because of to their strong surface plasmon resonance (SPR) properties and high biochemical activity.[4,5] Many studies utilized the color change resulting from the aggregation and dispersion of AuNPs to realize highly sensitive biosensors. Liu *et al.* proposed an aggregation of single-chain variable fragment (scFv) stabilized AuNPs to detect rabbit IgG.[6] Yuan *et al.* developed a novel AuNPs biosensor based on the aggregation of AuNPs caused by increasing salt concentration.[7] Xu *et al.* utilized the antibody modified with Au nanorods for the conjugation with the detection target, alpha-fetoprotein, resulting in aggregation of nanorods.[8] Although AuNPs exhibit obvious color, the commercial AuNPs are still too expensive, which leads to high-cost biosensors.

In this study, a novel biosensor was developed based on high absorption and high scattering nanostructured materials to enhance the optical signal. Carbon nanotubes (CNTs) were used as a label material to demonstrate the feasibility owing to the fact that CNTs exhibit non-resonant structures that can give broadband absorption.[9–11] Besides, CNTs provide high light-scattering ability to enhance optical opacity.[12] Moreover, CNTs are less costly than AuNPs which can significantly reduce the cost of biosensor. Human serum albumin (HSA) was selected as a detection target for its importance as a biomarker of liver and kidney function.[13] This is the first time to report that CNTs can be used to label HSA for detection characterized by UV-Vis and shows the potential of colorimetric detection by naked-eye.

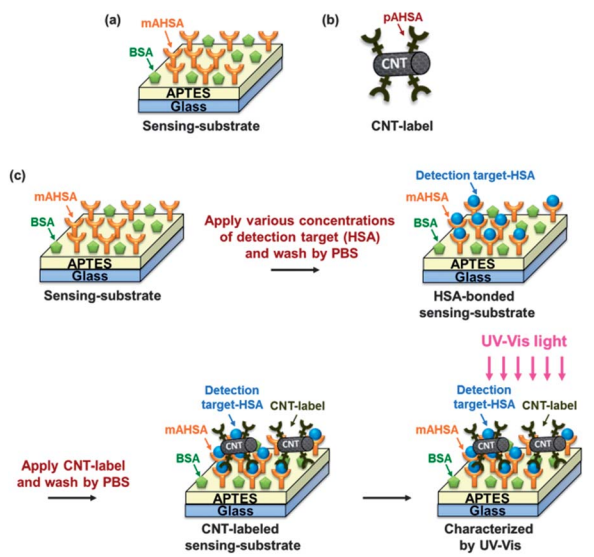

Scheme 1 Schematics diagram of the biosensor system including (a) a sensing-substrate and (b) a CNT-label. (c) Schematic diagrams for the operation flow of HSA detection using this biosensor.

National Tsing Hua University, Department of Materials Science and Engineering, 101, Sec. 2, Kuang-Fu Road, Hsinchu, Taiwan 30013. E-mail: tryew@mx.nthu.edu.tw; Fax: +886-3-5722366

† Electronic supplementary information (ESI) available: Experimental details and additional data are supplied as the ESI. See DOI: 10.1039/c3tb20980f

The biosensor is composed of two components, a sensing-substrate (Scheme 1a) and a CNT-label (Scheme 1b), respectively. The sensing-substrate is made of a piece of glass with the surface modified with bovine serum albumin (BSA, sigma, B2518)/monoclonal anti-human serum albumin (mAHSA, abcam, ab18083)/3-aminopropyltriethoxysilane (APTES, Alfa Aesar, A10668), as described by the previous work to provide specific binding to human serum albumin (HSA, abcam, ab67670).[14] The CNT-label is composed of CNTs which were immobilized with polyclonal AHSA (pAHSA, abcam, ab24207) to label the detected HSA on the sensing-substrate. The detection process is shown in Scheme 1c and briefly described as following. HSA was immobilized on the sensing-substrate and then bonded with the CNT-label from the final structure, CNT-labeled sensing-substrate, whose optical tramission was measured by UV-Vis (Cary 60) (Experimental details are listed in the ESI†).

To ensure the specific HSA-detection of the biosensor, the sensing-substrate was functionalized with mAHSA and BSA. Therefore, the immobilization of the mAHSA on the APTES-modified glass, and the blocking of BSA on untreated and non-specific bonding sites before HSA sensing should be confirmed. These could be verified by applying the goat polyclonal secondary antibody to mouse IgG with fluorescein isothiocyanate (anti-IgG–FITC, abcam, ab6785) to the sensing-substrate as described in previous work.[14] As shown by the fluorescence images in ESI (Fig. S1a–1d†), the success of mAHSA immobilization and the BSA blocking on the APTES-modified glass have been verified.

After the various concentrations of HSA were applied on the sensing target, it is important to ensure the success of HSA conjugation with the mAHSA on the sensing-substrate which can be verified by applying rabbit polyclonal to HSA with FITC (AHSA–FITC, abcam, ab34669), and schematics diagram as shown in Fig. 1a. Fig. 1b–1d show green fluorescence images of the sensing-substrate applied with AHSA–FITC, and after the addition of HSA in concentrations of 2×10^{-4}, 2×10^{-2}, and 2×10^{-1} mg ml^{-1}, respectively. The figures show that the intensity of fluorescence rises with the increase in HSA concentration, indicating that the detection target HSA was conjugated on the sensing-substrate successfully.

The morphology of COOH-modified CNTs used in this study is shown in the scanning electron microscope (SEM) image in Fig. 2a. The length and diameter of COOH-modified CNTs are 0.5–2 μm and about 20 nm, respectively. In addition, the CNT-label should be stored in buffer solution with pH = 7.4 to maintain its activity. To ensure the well-dispersion of COOH-modified CNTs in buffer solution, four common buffer solutions PBS, buffer solution (KH_2PO_4 (0.2 g L^{-1}) and Na_2HPO_4 (1.16 g L^{-1})), Hank's Balanced Salt Solution (HBSS), and tris(hydroxymethyl)aminomethane hydrochloride (Tris–HCl), were tested in this work (please see ESI Fig. S2† for detailed results and description). The results indicated that the buffer solution was experimentally verified for better CNT dispersion than others and was used in this work. The COOH-modified CNTs was still dispersed well in buffer solution after being stored statically for 24 h, as shown in Fig. 2b.

As the CNT-label was utilized as a label material for HSA detection, it is important to verify the success of the cross-linking between pAHSA and COOH–CNTs after EDC–NHS reaction. The cross-linking condition can be determined by applying the anti-IgG–FITC onto the CNT-label. The detailed results and description are shown in ESI (Fig. S3a–3e†) and the schematics diagram is shown in Fig. 2c. The brightest fluorescence image showed that the optimum condition for the cross-linking of pAHSA with COOH-modified CNT was 250 mM EDC and 100 mM NHS, as shown in Fig. 2d (same as Fig. S3d†).

Fig. 3a showed the transmission spectra of the sensing-substrate. The mean transmission value at 400 nm for the ten specimens was 95.8% and the relative standard deviations (R.S.D.) are less than 0.5%. This indicated that the process of fabrication the sensing-substrate had an excellent reproducibility. Therefore, the transmission value was viewed as a constant within the various sensing-substrate specimens. To characterize the sensing module of the biosensor, the transmission spectra of the biosensor were monitored between

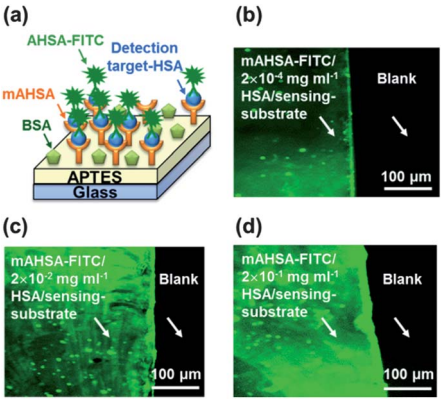

Fig. 1 The (a) schematic diagram and fluorescence images with AHSA–FITC conjugated on the sensing-substrate applied with the HSA concentrations of (b) 2×10^{-4}, (c) 2×10^{-2}, and (d) 2×10^{-1} mg ml^{-1}.

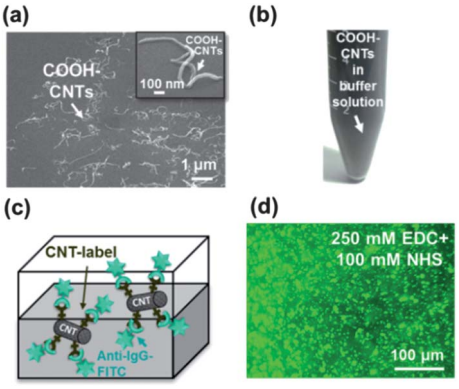

Fig. 2 (a) The SEM images of COOH-modified CNTs on a hydrophilic glass substrate. (b) The photo image of CNTs well-dispersed in buffer solution after being stored statically for 24 h. The (c) schematic diagram and (d) fluorescence image of the anti-IgG–FITC conjugated on CNT-label which was immobilized with pAHSA.

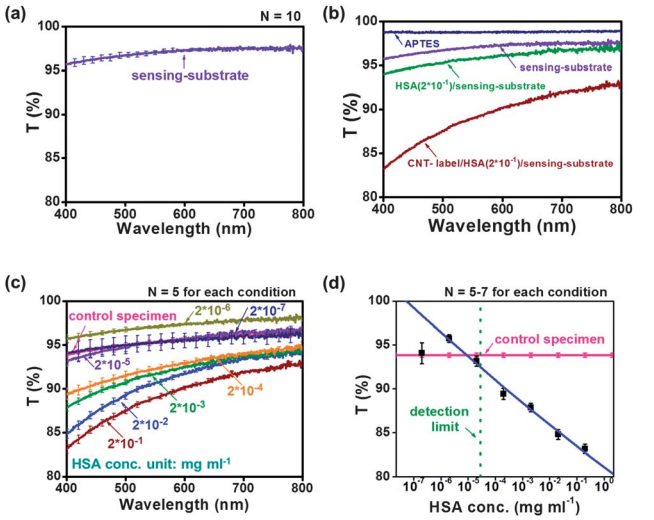

Fig. 3 (a) The UV-Vis transmission spectra of the sensing-substrate. (b) The plot of transmission value *versus* wavelength at the HSA concentration of 2×10^{-1} mg ml^{-1}. (c) The CNT-labeled sensing-substrate with various concentrations of HSA which were 0, and from 2×10^{-7} to 2×10^{-1} mg ml^{-1}, respectively. (d) The plot of transmission measured at 400 nm *versus* different HSA concentrations.

process steps, including after APTES modification, after mAHSA and BSA immobilization (sensing-substrate), and HSA conjugation. Taking the concentration of HSA of 2×10^{-1} mg ml^{-1} as an example, Fig. 3b showed the transmission spectra which were measured by UV-Vis. The spectra showed that the transmission was only significantly reduced after applying the CNT-label on the HSA-bonded sensing-substrate. Accordingly, the single transmission measurement of the biosensor was done at the CNT-labeled sensing-substrate with various HSA concentrations.

Fig. 3c showed the transmission spectra of the CNT-labeled sensing-substrate with the HSA concentrations of 0 and 2×10^{-7} to 2×10^{-1} mg ml^{-1}. The CNT-labeled sensing-substrate without HSA (HSA concentration: 0 mg ml^{-1}) served as the control specimen. The measured transmission value of 93.9% was considered as the background level which sets the detection limit of the biosensor demonstrated in this work. It can be observed that there is a consistent reduction of transmission with increasing HSA concentrations. To ensure the reproducibility and consistency of this biosensor, five different samples for each HSA concentration prepared at different time were measured ($N = 5$). The relative standard deviations (R.S.D.) of the transmission spectra measured by UV-Vis shown on Fig. 3c are all less than 2%, which indicates good reproducibility. Furthermore, to quantify the HSA concentrations, the transmission signals were measured at the wavelength of 400 nm, the most significant changes of the transmission spectra, after CNT-labeled sensing-substrate with the HSA concentrations ranging from 2×10^{-7} to 2×10^{-1} mg ml^{-1}. The reduction optical transmission is mainly contributed by CNTs bound on the substrates because of their high absorption coefficient and the high scattering ability. As shown in Fig. 3d, the transmission ratio is linear to the HSA concentration, ($N = 5$–7) for each HSA ranging from 2×10^{-5} to 2×10^{-1} mg ml^{-1} in log-scale, with a corresponding regression equation ($\log y = 1.91$–$0.01 \log x$, $R^2 = 0.988$). The horizontal dash line in Fig. 3d shows the average transmission value of the control specimen discussed above. This suggests the detection limit of the biosensor for HSA detection is approximately 3×10^{-5} mg ml^{-1}. Compared with other nanostructure-based immunoassay biosensors which also use UV-Vis for detection, this biosensor exhibits higher sensitivity and wider detection range than gold nanostructure biosensors.[6–8,15] Besides, this approach provides an innovative mechanism to detect antigen instead of applying SPR properties. The above results demonstrate the feasibility of using nanostructured material with high absorption and high scattering ability as a label material for biosensor that can quantify antigen concentration, achieve high sensitivity and wide detection range for biosensor application.

Moreover, the various transmission values with different HSA concentrations observed in the UV-Vis suggested the feasibility of directly capture these colorimetric changes by the naked eye for detection. After stacking three same specimens, the color difference at higher concentration of HSA could be observed visually as shown in Fig. 4. This visual result demonstrated that this sensor bares the potential for daily life health check-ups through direct observation by the user, hopefully, as convenient as today's off-the-counter pregnancy test kits.

Fig. 4 The images of biosensors (after stacking three specimens in the same condition) with various concentrations of HSA of 2×10^{-1}, 2×10^{-2}, 2×10^{-3} and 0 mg ml^{-1}, respectively.

Conclusions

This study first developed a novel biosensor for HSA detection by utilizing a label material with high absorption coefficient and high light scattering ability. The biosensor using CNT as a label for HSA detection was demonstrated successfully. The calibration results show good linearity between HSA concentration and reduction in optical transmission. The biosensor shows the following advantages. First, the high sensitivity for HSA detection with a detection limit of 3×10^{-5} mg ml^{-1} and wide detection range of 2×10^{-1} to 2×10^{-5} mg ml^{-1}. Second, the cost of the biosensor is reduced by using CNTs as a label material rather than AuNPs. Third, the biosensor could be operated in broad light wavelength range without the limitation of specific wavelength and shows the same performance for detection. Fourth, the colormetric biosensor could be detected by direct observation, because the color changed with different concentration of HSA. With further investigation on the real serum samples, interference and stability study, it is believed that this biosensor exhibit high potential in daily life use.

Notes and references

1 W. Rittenour, R. Hamilton, D. Beezhold and B. Green, *J. Immunol. Methods*, 2012, **383**, 47.
2 D. Tang, Y. Cui and G. Chen, *Analyst*, 2013, **138**, 981.
3 X. Pei, B. Zhang, J. Tang, B. Liu, W. Lai and D. Tang, *Anal. Chim. Acta*, 2013, **758**, 1.
4 E. E. Bedford, J. Spadacechia, C. M. Pradier and F. X. Gu, *Macromol. Biosci.*, 2012, **12**, 724.
5 K. Saha, S. S. Agasti, C. Kim, X. Li and V. M. Rotello, *Chem. Rev.*, 2012, **112**, 2739.
6 Y. Liu, Y. Liu, R. L. Mernaugh and X. Zeng, *Biosens. Bioelectron.*, 2009, **24**, 2853.
7 Y. Yuan, J. Zhang, H. Zhang and X. Yang, *Biosens. Bioelectron.*, 2011, **26**, 4145.
8 X. Xu, Y. Ying and Y. Li, *Sens. Actuators, B*, 2012, **175**, 194.
9 Z. P. Yang, L. Ci, J. A. Bur and S. Y. Lin, *Nano Lett.*, 2008, **8**, 446.
10 K. Mizuno, I. Ishii, H. Kishida, Y. Hayamizu, S. Yasuda, D. N. Futaba, M. Yumura and K. Hata, *Proc. Natl. Acad. Sci. U. S. A.*, 2009, **106**, 6044.
11 M. S. Haque, U. F. Claudio Marinelli and W. I. Milne, *NSTI Nanotech 2006, NSTI Nanotechnol. Conf. Trade Show*, 2006, **1**, 134.
12 G. E. Jonsson, H. Fredriksson, R. Sellappan and D. Chakarov, *Int. J. Photoenergy*, 2011, **2011**, 939807.
13 K. H. Ulrich, V. T. G. Chuang and M. Otagiri, *Biol. Pharm. Bull.*, 2002, **25**, 695.
14 M. C. Tu, Y. T. Chang, Y. T. Kang, H. Y. Chang, P. Chang and T. R. Yew, *Biosens. Bioelectron.*, 2012, **34**, 286.
15 S. B. Zhang, Z. S. Wu, M. M. Guo, G. L. Shen and R. Q. Yu, *Talanta*, 2007, **71**, 1530.

